Adaptive Active Power Sharing Techniques for DC and AC Voltage Control in a Hybrid DC/AC Microgrid

Ángel Navarro-Rodríguez, Pablo García, Ramy Georgious and Jorge García
Dept.of Electrical, Electronics, Systems & Computers Engineering
University of Oviedo, LEMUR Group
Gijón, 33204, Spain
Email: navarroangel@uniovi.es, garciafpablo@uniovi.es, georgiousramy@uniovi.es, garciajorge@uniovi.es

***Abstract*—This paper deals with the AC and DC dynamic voltage control in a hybrid DC/AC Microgrid (MG) with central and distributed Battery Energy Storage Systems (BESSs), applying a power sharing mechanism between the different devices in the MG. The MG is composed by a multiport transformation center and two fixed frequency 3 phase AC Nanogrids (NGs) coupled to a DC bus through 3-phase Power Electronic Converters (PECs). The system pursues to minimize the dependence on the utility grid, the needed DC capacitance and the stress in the MGs central BESS, while increasing the power handling capability and the overall system stability during islanding condition. In order to approach the proposed aim, two main concerns are studied in this paper: an adaptive power sharing mechanism between the DC bus and the AC NGs for DC voltage control, and the design and implementation of an AC dynamic local voltage compensator based on Distributed Energy Storage System (DESS).**

I. Introduction

The increasing concern about environmental issues and the rising popularity of concepts as local generation and self-consumption have led to an increasing interest on alternatives to the conventional utility grid as Microgrids (MGs), Nanogrids (NGs) and Smart grids (SGs). Despite its advantages, the weakness and stability problems associated to a MG have been considered since its apparition, demanding significant research interests. Studies for different types of contingencies have been carried out, pursuing the power quality improvement [1], [2]. Furthermore, with the apparition of hybrid DC/AC MGs, where the Power Electronic Converters (PECs) may share power not only in the AC grid but also in the DC lines, new MG issues appears as the stability and quality maintenance in both DC and AC [3]–[5].

Different methods and control topologies have been presented in the literature to ensure the distribution network (DN) voltage control and power flow, as the central controller, the master-slave, the Q/V and P/f droops, and hybrid approaches [6]–[9]. The fast development of power semiconductor devices and digital control systems have made PECs the most suitable interface for both generation, Energy Storage Systems (ESS) and loads leading to MGs dominated by PECs. Moreover, due to the high penetration of renewable generation operating at its maximum power point tracking (MPPT), the control methods based on master-slave or multiple slack, with fixed frequency in the case of AC, can simplify the MGs design [10]–[12].

Concerning the dynamic active power sharing improvement in AC grids, many studies can be found in the literature based on the variation of the frequency with the active power (P/f droop), being the stiffness determined by the system inertia [13]–[16]. However, when the fixed frequency approach is used instead, active power variations will affect the voltage magnitude (P/V droop) being the grid inertia dependent on the grid equivalent capacitance. Regarding the dynamic power sharing between hybrid AC/DC MGs when AC slack converters are used for the coupling between the Low Voltage DC line (LVDC) and the AC grid, few discussion is found in the literature. Some studies have been proposed based on cascaded converters stability [17], and power balancing between AC and DC using a V_g/V_{dc} droop [18]. However, these methods have been proposed for AC/DC/AC grid tied converters and they can not be directly applied to the AC/DC voltage control of a hybrid MG.

Thus, this paper deals with the AC and DC voltage control in a hybrid DC/AC MG with central and distributed Battery Energy Storage Systems (BESSs). A power sharing mechanism between the different distributed energy resources (DERs) is proposed. The system will have as main constraints the reduced dependency on the main grid, the islanded operation and the optimization of the ESS usage. Two main concerns are studied in this paper: 1) designing an adaptive method for the dynamic power sharing between the DC bus and the AC NGs for an enhanced DC voltage control; and 2) the implementation of an AC voltage compensator for the NG-based distribution system. The compensation will relay on the use of virtual capacitor for an improved system stiffnesss.

The present work has been partially supported by the predoctoral grants program Severo Ochoa for the formation in research and university teaching of Principado de Asturias PCTI-FICYT under the grant ID BP14-135. This work also was supported in part by the Research, Technological Development and Innovation Program Oriented to the Society Challenges of the Spanish Ministry of Economy and Competitiveness under grant ENE2016-77919-R and by the European Union through ERFD Structural Funds (FEDER).

The paper is organized as follows. Section II introduces the proposed hybrid DC/AC Microgrid topology. Section III explains the basics of the proposed voltage control loops in DC and AC systems. Section IV covers the proposed adaptive voltage control in the hybrid DC/AC MG. Finally, section V presents the simulation results.

II. The proposed hybrid DC/AC MG

The hybrid MG under study, shown in Fig. 1, is composed by a MG transformation center (MGTC) and two 3-phase AC NGs based on fixed frequency Master-Slave topology. The MGTC consists of a BESS and a connection to the main grid interconnected by a common Low Voltage DC bus (LVDC) to two NG Head Converters (NGHCs) feeding the AC NGs. The BESS and main grid are interfaced with the LVDC by a three-port solid-state transformer (SST). It is worth to point out that the SST operation is out of the scope of this paper. The MG is designed as follows. The NGHC acts as an slack, both for the AC voltage magnitude and frequency. The MGs loads, Constant Power Loads (CPLs) and Constant Impedance Loads (CILs), are only located at the 3 phase NGs. Under this configuration, the load as seen by the LVDC is drawn by the NGHCs. Additionally, different distributed resources such as Distributed Generation (DG) and ESSs can be installed at NG level. A central controller governs the MGTC and low bandwidth communications are considered in the NGs between the DGs, ESSs and NGHCs.

Power mismatches in conventional grids are absorbed by the high inertia of generators. However, in the case under study, they have to be supported by the energy storage elements, including capacitances, installed at the MG. As a first approach, DGs and DESS in the NG will operate with constant PQ commands while the slack NGHCs will absorb the power transients, controlling the voltage magnitude and frequency. Additionally a local dynamic voltage compensator able to share active power might be considered in the NGs. Depending on the MG being connected/disconnected to the main grid, two modes of operation are defined: 1) During *non-islanding* operation, the utility grid P_{main} and the BESS P_{BESS} can share the effort; 2) During *islanding*, the proposed MG is disconnected from the utility grid and only the BESS is available as a power source in the transformation center.

In any case, the voltage in DC and AC NGs should remain under control within regulation limits. Additionally, two constraints are established: 1) The dependence on the utility grid should be minimized; 2) The BESS limitations (Bandwidth, available power, State of Charge (SoC)) have to be considered in the power sharing. This paper is focused on the operation during *islanding* mode.

Although the DGs in the NG could be used to provide ancillary services, most of DERs in the NG either present a low response or should be operated in Maximum Power Point Tracking (MPPT). However, DESSs in the NG can be used, providing local compensation while reducing the conduction losses. As a first approach, in this study one local ESSs will

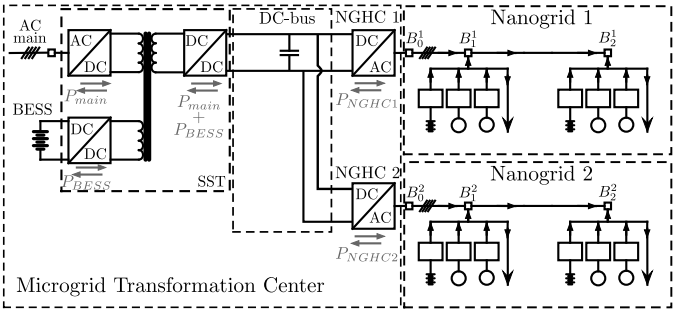

Fig. 1. Topology of the Hybrid DC/AC Microgrid under study.

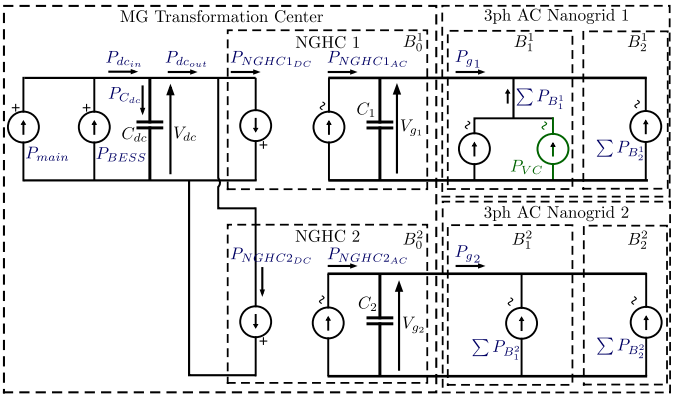

Fig. 2. Simplified power sharing scheme within the Hybrid DC/AC MG.

be used for transient compensation located at the first node of NG1 (B_1^1). Fig. 2 shows a simplified scheme of the MG illustrating the different elements participating on the power sharing, where $\sum P_{B_j}^k$ (k denotes the NG, while j the node) is the total power share between DGs, DESS and active power loads within a node, $\sum P_{B_j}^k = \sum(P_{DG_j}^k + P_{DESS_j}^k - P_{L_j}^k)$.

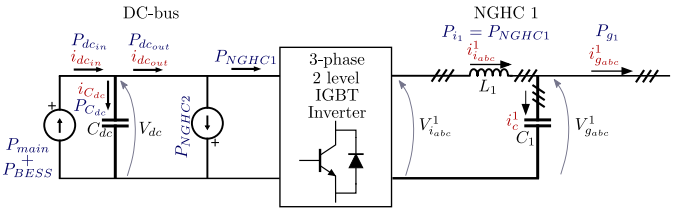

Fig. 3. Simplified equivalent power scheme of one of the NGHCs.

The system model for the voltage control, both in AC and DC, is simplified to a capacitor, neglecting line impedances and approximating the current control loops of the PECs to a low pass filter (LPF). 3-phase balanced AC NGs are assumed.

The modeling of the proposed system will be based on the simplified power scheme for one of the NGHCs shown in Fig. 3. Thus, the AC system modeled in dq synchronous reference frame is defined by (1), where k is the NG identifier, v_g^k is the NG voltage at node B_0^k, i_i^k is the current drawn by the NGHCs into the NGs (i.e. the control action of NGHCs), ω_e^k is the grid frequency and i_g^k is the total current drawn by the

$$\frac{d}{dt}\begin{bmatrix} i^k_{i\,d} \\ v^k_{g\,d} \\ i^k_{i\,q} \\ v^k_{g\,q} \end{bmatrix} = \begin{bmatrix} \frac{-R_k}{L_k} & \frac{1}{L_k} & 0 & 0 \\ \frac{1}{C_k} & 0 & 0 & 0 \\ 0 & 0 & \frac{-R_k}{L_k} & \frac{1}{L_k} \\ 0 & 0 & \frac{1}{C_k} & 0 \end{bmatrix} \begin{bmatrix} i^k_{i\,d} \\ v^k_{g\,d} \\ i^k_{i\,q} \\ v^k_{g\,q} \end{bmatrix} + \begin{bmatrix} \omega^k_e & 0 & 0 & 0 \\ 0 & \omega^k_e & 0 & 0 \\ 0 & 0 & -\omega^k_e & 0 \\ 0 & 0 & 0 & -\omega^k_e \end{bmatrix} \begin{bmatrix} i^k_{i\,q} \\ v^k_{g\,q} \\ i^k_{i\,d} \\ v^k_{g\,d} \end{bmatrix} + \begin{bmatrix} \frac{1}{L_k} & 0 & 0 & 0 \\ 0 & \frac{-1}{C_k} & 0 & 0 \\ 0 & 0 & \frac{1}{L_k} & 0 \\ 0 & 0 & 0 & \frac{-1}{C_k} \end{bmatrix} \begin{bmatrix} v^k_{g\,d} \\ i^k_{g\,d} \\ v^k_{g\,q} \\ i^k_{g\,q} \end{bmatrix} \quad (1)$$

buses B^k_1 and B^k_2, i.e., the system disturbance.The DC link can be modeled in terms of active power as (2), where C_{dc} is the LVDC capacitor, P_{dcin} is the power shared by the main and the central BESS, and P_{dcout} is the power drawn by the NGHCs ($P_{dcout} = P_{NGHC_1(t)} + P_{NGHC_2(t)}$), being defined by (3), assuming $v_{g_q} = 0$. Thus, the NGHCs are seen as CPLs by the DC link. The power flowing into the capacitor is defined as $P_{C_{dc}} = P_{dcin} - P_{dcin}$.

$$\frac{dV_{dc(t)}}{dt} = \frac{1}{C_{dc}V_{dc(t)}}\left(P_{dcin} - \underbrace{\left(P_{NGHC_1(t)} + P_{NGHC_2(t)}\right)}_{P_{dcout}}\right) \quad (2)$$

$$P_{dcout_{(t)}} = \sum_{k=1}^{2} P_{NGHC_k(t)} = \sum_{k=1}^{2} \frac{3}{2}\left(v^k_{g\,d(t)} i^k_{i\,d(t)}\right) \quad (3)$$

III. Voltage Control: Controller Design

The MGTC control will involve the dynamic control of both DC link and AC NGs voltages. The closed loop voltage controllers, both in AC and DC, will be based on a feedback PI regulator. Two alternatives for the basic voltage control are considered in this paper. Fig. 4 shows the generic representation of those alternatives valid for both DC and AC voltage control, where $I_{L(t)}$, $P_{L(t)}$ and $G_{L(t)}$, are the time dependent disturbances drawn by constant current loads/generation (CCLs), constant power loads/generation (CCLs) and constant impedance loads/generation (CCLs) respectively. According to

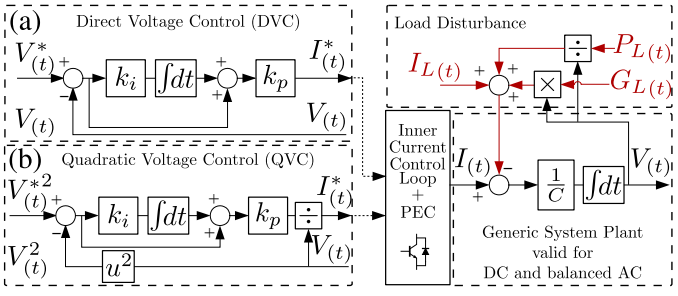

Fig. 4. Voltage control schemes, based on cascaded control, valid for the DC bus and the AC NGHCs. (a) conventional voltage control, namely DVC; (b) proposed alternative, QVC

this, the system plant is defined by (4), defining a non-linear system.

$$\frac{dV_{(t)}}{dt} = \frac{1}{C}\left(I_{(t)} - \underbrace{\left(I_{L(t)} + \frac{P_{L(t)}}{V_{(t)}} + G_{L(t)}V_{(t)}\right)}_{Disturbance}\right) \quad (4)$$

According to this expression, the conventional voltage control, referred in this paper as Direct Voltage Control (DVC), will present a non linear behavior under the presence of CGLs and CPLs. The use of an alternative control based on squared voltage is proposed for the system in this paper. Although it has been proposed before in the literature referred as energy based controller, its applications has been limited to the DC link control of DC/AC converters [19], [20]. Nonetheless, its application can be generalized to any cascade-based voltage control as slack converters in both DC and AC MGs. It will be referred as quadratic voltage control (QVC) in this paper. The QVC is defined by (5), valid for both AC and DC applications.

$$P^*_{(t)} = k_p({V^*_{(t)}}^2 - V^2_{(t)}) + k_i \int ({V^*_{(t)}}^2 - V^2_{(t)})dt \quad (5)$$

Where k_p and k_i are the ideal PI regulator gains. Despite the fact that the QVC also presents a non-linear relation between the voltage and the load disturbance, the relation between the square voltage and the CPLs is linear considering the system plant in (6), where P^* is the control action and $P_{c(t)}$ is the power flowing into the capacitor.

$$V_{(t)}\frac{dV_{(t)}}{dt} = \frac{1}{C}P_{c(t)} \Rightarrow \frac{dV^2_{(t)}}{dt} = \frac{2}{C}P_{c(t)} \quad (6)$$

The main feature of the voltage control for the application presented in this paper is the disturbance rejection capability. In order to analyze how the disturbance rejection of each method is affected by the type of load, their disturbance rejection transfer functions are obtained by linearization. The expressions for the DVC are shown in (7), (8) and (9).

$$\frac{\Delta V_{(s)}}{\Delta I_{L(s)}} \approx \frac{-sV_0^2}{s^2V_0^2C + sk_pV_0^2 - P_{L0} + G_{L0}V_0^2 + k_ik_pV_0^2} \quad (7)$$

$$\frac{\Delta V_{(s)}}{\Delta P_{L(s)}} \approx \frac{-sV_0}{s^2V_0^2C + sk_pV_0^2 - P_{L0} + G_{L0}V_0^2 + k_ik_pV_0^2} \quad (8)$$

$$\frac{\Delta V_{(s)}}{\Delta G_{L(s)}} \approx \frac{-sV_0^3}{s^2V_0^2C + sk_pV_0^2 - P_{L0} + G_{L0}V_0^2 + k_ik_pV_0^2} \quad (9)$$

Where V_0, P_{L0} and G_{L0} are the voltage magnitude , the CPL level, and the CIL level at the equilibrium point respectively.

The expressions for the QVC are stated in (10), (11) and (12), where I_{L0} is the CCL level at the equilibrium point.

$$\frac{\Delta V_{(s)}}{\Delta I_{L(s)}} \approx \frac{-sV_0}{s^2V_0C + s2k_pV_0 + I_{L0} + 2G_{L0}V_0^2 + 2k_ik_pV_0^2} \quad (10)$$

$$\frac{\Delta V_{(s)}}{\Delta P_{L(s)}} \approx \frac{-s}{s^2 V_0 C + s2k_p V_0 + I_{L0} + 2G_{L0}V_0^2 + 2k_i k_p V_0^2} \tag{11}$$

$$\frac{\Delta V^3{}_{(s)}}{\Delta G_{L(s)}} \approx \frac{-sV_0^2}{s^2 V_0 C + s2k_p V_0 + I_{L0} + G_{L0}V_0^2 + 2k_i k_p V_0^2} \tag{12}$$

These expressions demonstrate a clear dependency of the disturbance rejection transfer functions on the CPL, CIL and CCL levels in both the DVC and QVC. However, the DVC presents a critical negative dependency on CPL level, P_{L0}, for any kind of load disturbance, which can compromise the system stability. On the contrary, the QVC eliminates the dependency on CPL level. Due to the high presence of PECs, CPLs and constant power generation expected in the grid under analysis, a control based on the QVC is proposed for the application presented in this paper.

In order to tune the voltage regulator, a tunning method based on the linearized reference tracking transfer function is used. Applying linearization, the close loop system defined by (5) and (6) can be approximated as (13), where V_0^* and V_0 are the voltage reference and the voltage in the equilibrium point respectively. Considering operation near the equilibrium point and $V_0^* = V_0$, (13) can be approximated by a second order system with a determined natural frequency ω_n and a damping factor ξ as (14). Thus, the PI regulator gains of QVC are tunned according to (15). The natural frequency ω_n, should be selected according to the cascaded control premises, while the damping factor, xi, can be selected as a trade-off between overshoot and settling time.

$$\frac{V_{(s)}}{V^*_{(s)}} \approx \frac{s2k_p V_0^* + 2k_p k_i V_0^*}{s^2 C V_0 + s2k_p V_0 + 2k_p k_i V_0} \tag{13}$$

$$\frac{V_{(s)}}{V^*_{(s)}} \approx \frac{2\xi\omega_n s + \omega_n^2}{s^2 + 2\xi\omega_n s + \omega_n^2} \tag{14}$$

$$k_p = \xi\omega_n C;\ k_i = \frac{\omega_n^2 C}{2k_p} \tag{15}$$

A. QVC applied to DC voltage control

The described QVC scheme can be applied directly as shown in 4(b), considering the control action of the PI regulator as the active power reference required by the DC bus capacitor. The specific basic DC bus voltage control is shown in Fig. 5. As specified before, during *non-islanding* both the BESS and the main grid participate in the control. To reduce the dependence on the main grid, the BESS provides the low bandwidth variations, within its power limitations, while the main contribute with the high bandwidth transients unless the battery power is limited for any reason, in which case the main will participate also in the steady state. In the case of *islanding*, the battery would be the only available power source to maintain the regulation of the DC link. In that case, to maintain the proper operation of the voltage regulator, either a back calculation or a reduction on the control bandwidth, ω_n, should be applied to fulfill the cascaded control requirements.

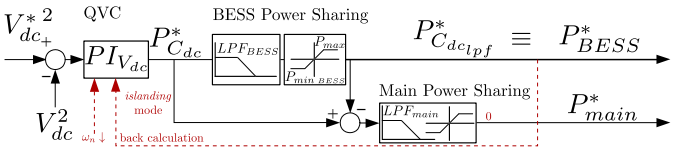

Fig. 5. DC bus slack controller based on Quadratic Voltage Control. *islanding* mode modifications highlighted in red.

B. QVC applied to 3-phase AC voltage control

In the case of AC, a voltage control in the *dq* reference frame is proposed based on QVC and fixed frequency. The complete cascaded control scheme for a 3-phase AC slack converter is shown in Fig. 6. A grid current decoupling term could be added in order to improve the disturbance rejection response, drawn in green color. However, an improved disturbance rejection could increase the stress in the DC side for the proposed MG topology, which is translated in an increased stress in the BESS during an *islanding* scenario.

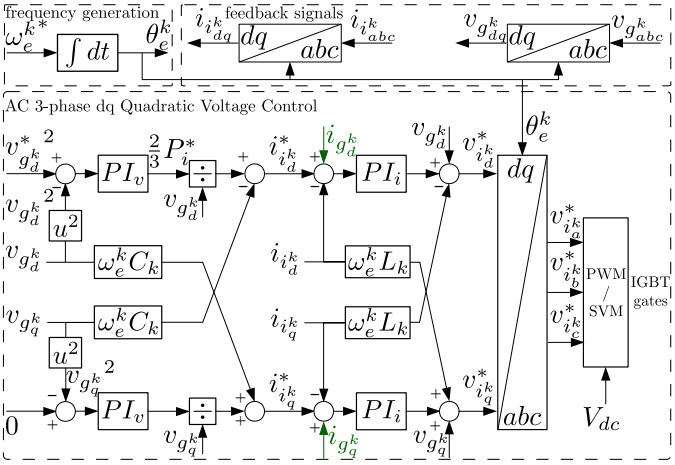

Fig. 6. NGHCs basic AC slack controller based on AC quadratic voltage control implemented in the dq reference frame.

IV. Hybrid DC/AC voltage control: Adaptive Power Sharing in the LVDC and Local Dynamic Voltage Compensation in the AC NGs

The proposed hybrid MG should maintain the power quality and reliability in both the LVDC bus and the AC NGs. This paper deals with the specific task of managing the dynamic active power sharing between the elements present in the grid in order to keep the voltage magnitude quality, and the frequency in the case of the AC NGs. The proposed power topology allows to decouple the events and contingencies happening in the LVDC bus from the voltage control in the NGs, as long as the DC voltage remains within certain levels. However, the NGHCs control is not decoupled from the

LVDC, being the last one subjected to any disturbance taking place in the NGs. During *islanding*, this control scheme leads to the battery and the DC link capacitor absorbing/injecting any power mismatch within the NGs. In order to soften this effect a coupled hybrid control is proposed as follows.

A. The DC bus voltage control scheme

The proposed DC bus voltage control scheme is defined as shown in Fig. 7. It consists on a QVC controller generating a power reference $P^*_{C_{dc}}$. In order to limit the stress on the central BESS and comply with its limitations (bandwidth or instantaneous power), $P^*_{C_{dc}}$ is divided into a low ($P^*_{C_{dc_{lpf}}}$) and high ($P^*_{C_{dc_{hpf}}}$) bandwidth components by using low pass filters and saturation. The low frequency command $P^*_{C_{dc_{lpf}}}$ will be given by the BESS, whereas the $P^*_{C_{dc_{hpf}}}$ command will be share by the utility grid (if available) and the NGHCs, $P^*_{NGHC_k}$. As *islanding* mode is assumed in this paper, the utility grid power command $P^*_{main} = 0$. It is worth noting that adjusting the power drawn by the NGHCs by commanding a $P^*_{NGHC_k}$ will lead to an adverse effect in the AC NGs voltage controller, being necessary to pursue for a trade-off between the DC and AC NGs quality based on the conditions of each NG. The power shared between the NGHCs will be defined by an adaptive algorithm based in the DC and AC NGs parameters and instantaneous conditions. As a first approach, the DC and AC voltage deviations from their references will be used. The proposed algorithm is expressed by equations (16) and (17). First, a sharing coefficient (σ_k) is obtained for each NGHC (16), where ΔV_{dcpu} and $\Delta V_{gk_{pu}}$ are the DC and AC NGs voltage variations in p.u., λ_{dc} and λ^k_{ac} are weighting factors and K_{ish} is an integral gain. The integral is saturated between 0 and 1. After, the commanded power to each NG is normalized according to its sharing coefficient and the summation of all the coefficients from the different NGs (σ^k_n) (17).

$$\sigma_k = k_{ish} \int (\lambda_{dc} \Delta V_{dcpu} - \lambda_{ac_k} \Delta V_{ac_k pu}) dt \qquad (16)$$

$$P^*_{NGHC_k} = P_{dc_{hpf}} \underbrace{\frac{\sigma_k}{\sum_{i=1}^{2} \sigma_i}}_{\sigma^k_n} \qquad (17)$$

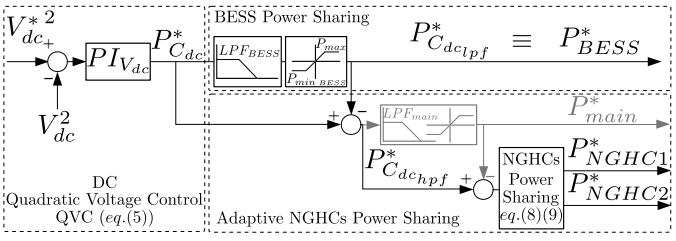

Fig. 7. Proposed hybrid DC/AC voltage control: DC voltage control scheme based on adaptive power sharing between the different elements in the MG transformation center.

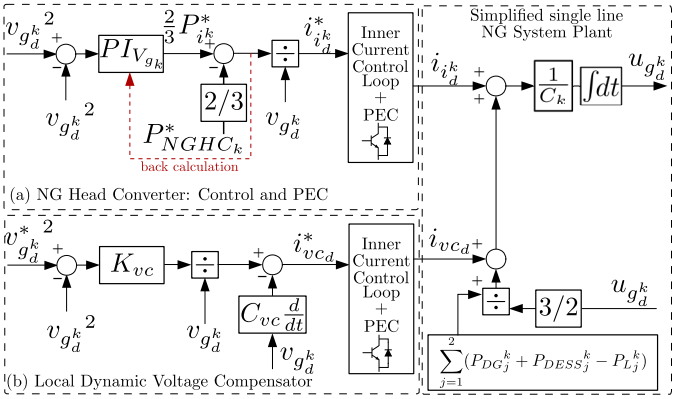

Fig. 8. Proposed hybrid DC/AC voltage control: decentralized AC NGs voltage control scheme. a) NGHC control; b) Local Dynamic Voltage Compensator.

B. The AC Nanogrids voltage control scheme

The proposed AC NG voltage control scheme is defined in Fig. 8. The control is implemented at the dq reference frame. As the main concern of this study is the active power sharing, this paper will be focus only in the control of d axis, assuming full decoupling from the q axis. The NGHC (Fig. 8(a)) will operate as a slack converter fixing the frequency and controlling the voltage magnitude in both transients and steady state. It consists on a QVC PI controller generating a power reference $P^*_{i^k}$. When the hybrid adaptive power sharing is enabled, the power reference $P^*_{NGHC_k}$ obtained by (17) is subtracted from $P^*_{i^k}$, modifying the control action. To prevent the voltage controller from eliminating the effect of $P^*_{NGHC_k}$, back calculation is applied. As the NGHC is the NG slack, a modification in its power reference will lead to a variation in the voltage magnitude, thus allowing the exchange of power between the DC and AC systems. However, this effect is subject to elements in the AC NG providing/absorbing power as a reaction to the voltage variation. This can be provided by the grid equivalent capacitance, enabling a limited participation during the transients, or by introducing ancillary services for such a purpose in the NG.

A solution to maintain the quality and increase the participation in the Hybrid DC/AC NG power sharing is to include local dynamic voltage compensation within the NG. It can be addressed by any local DG or DBESS available in the NG, able to provide active power. The proposed generic control topology for the local dynamic voltage compensator is shown in Fig. 8(b) and defined by (18). A virtual capacitance ($C_{vc}\frac{d}{dt}$ in the ideal form) increases the grid equivalent capacitance, enhancing the initial transient response and improving the participation during transients in the hybrid sharing mechanism. A P quadratic regulator (K_{vc}) improves the grid voltage damping, and enable the participation during steady state in the hybrid DC/AC power sharing. Both parts of the controller can be implemented independently or combined depending on

the limitations of the DG or DBESS providing that service.

$$i^*_{vc_{dq}(t)} = \underbrace{\frac{K_{vc_{dq}} \cdot \left(v^{*}_{g^k_{dq}(t)}{}^2 - v_{g^k_{dq}(t)}{}^2\right)}{v_{g^k_{dq}(t)}}}_{\text{damping factor}} \underbrace{-C_{vc} \cdot \frac{d}{dt} v_{g^k_{dq}(t)}}_{\text{Virtual Capacitor}} \tag{18}$$

V. Simulation Results

The proposed system has been validated through simulations in MATLAB/Simulink®. The parameters are summarized in Table I. Two scenarios are simulated to evaluate the performance of the control topology proposed in this paper compared with the original case. The first test applies the proposed adaptive technique for power sharing without the local voltage compensator, while in the second test a local voltage compensator is included in the first NG with the K_{vc} and C_{vc} parameters in Table I. The results are shown in Fig. 9 and 10 respectively. They show the DC voltage, the AC voltage in both NGs, the sharing coefficients, the power commands generated by the DC controller in Fig. 7 and the CPL in each NG. The original case consists on the control presented in Fig. 7 and 8 by dissabling the power sharing in DC ($\sigma^1_n = \sigma^2_n = 0$) and without local voltage compensation in the NGs. Considering a BESS bandwidth of 100Hz (Table I), in the original case the DC voltage control bandwidth is reduced to 20Hz in order to extend the system stability. On the contrary, when the proposed technique is applied the overall current bandwidth is 500Hz and the DC voltage controller bandwidth can be increased up to 50Hz. The system is tested under multiple steps of CPL disturbances in both NGs. In both tests, the proposed sharing technique (and the voltage compensator in the second case) is activated at $t = 0.3s$. Between $t = 0$ and $t = 0.3s$, the effect of using excessive voltage control bandwidth with reduced current bandwidth is illustrated. From $t = 0.3$ to $t = 0.7$ the proposed techniques are operating. As expected, the power required by the DC voltage controller is now shared between both NGs and central BESS, reacting one NG to the events on the other. As the BESS provides the steady state, the power shared operates only during the transients. In the first case, the DC voltage transients are improved compared to the original, however the AC NGs voltages are distorted as a consequence. In the second case, under the same conditions, the use of a local voltage compensator leads to an overall improvement in both DC and AC voltages, reducing significantly the voltage variations under CPL steps. At the instant $t = 0.7s$, the total system load exceeds the central BESS maximum power leading to an overall MG collapse in the first case and in the original (Fig. 9). On the other hand, the use of a local compensator not only improves the transients but also enables the sharing mechanism to operate during steady state. As shown in Fig. 10, once the BESS limits, the compensator start providing the power to maintain the DC and AC NGs stable at the expense of an stationary error in V_{g_1} caused by the P regulator in the local compensator.

TABLE I
System Parameters

AC Nanogrids Parameters	Values
AC Nominal Voltage (V^*_{g1}, V^*_{g2})	230 $V_{AC_{rms}}$/50Hz
NGHCs AC voltage control ω_n /xi	2π50 rad/s / 1
NGs equivalent Capacitor (C_1, C_2)	300 μF
AC Voltage compensator gains K_{vc} / C_{vc}	0.3/0.001
DC link Parameters	**Values**
DC Nominal Voltage (V^*_{dc})	700 V
DC Current control loop ω_{n_i}	2π500 rad/s
DC equivalent Capacitor (C_dc)	300 μF
DC Voltage control loop ω_n /xi	2π50 / 1
Central BESS BW / P_{max}	100 Hz / 17.5 kW
Power Sharing $k_{i_{sh}}$ / λ_{dc} / λ_{ac_1} / λ_{ac_2}	30 / 2 / 1 / 1

VI. Conclusions

In this paper, a dynamic voltage control technique is proposed for a fixed frequency hybrid AC/DC Microgrid with ESS, based on the power sharing between the AC NGs and a central BESS to maintain the grid quality in both the LVDC and the AC NGs with high penetration of CPLs and PECs. An adaptive power sharing mechanism have being presented for maintaining the LVDC voltage under control, not only reducing the stress in the central BESS system and the dependence in the utility grid but also demonstrating the extended operation and improved transient response in the LVDC when the central BESS presents bandwidth and power limitations. In addition, a local AC dynamic voltage compensator has been proposed for AC voltage control support based on virtual capacitance. The theoretical discussion has been supported with simulations. Further investigation on the local compensator tunning and effects, considering the use of adaptive techniques, the enhancement of the adaptive algorithm, considering other factors as the load level or the grid capacitance, and the experimental validation are part of an on-going research.

.

References

[1] J. M. Guerrero, "Editorial Special Issue on Power Electronics for Microgrids 2014;Part II," *IEEE Transactions on Power Electronics*, vol. 26, no. 3, pp. 659–663, March 2011.

[2] J. Guerrero, P. C. Loh, T.-L. Lee, and M. Chandorkar, "Advanced Control Architectures for Intelligent Microgrids 2014;Part II: Power Quality, Energy Storage, and AC/DC Microgrids," *IEEE Transactions on Industrial Electronics*, vol. 60, no. 4, pp. 1263–1270, April 2013.

[3] P. Wang, X. Liu, C. Jin, P. Loh, and F. Choo, "A hybrid AC/DC microgrid architecture, operation and control," in *Power and Energy Society General Meeting, 2011 IEEE*, July 2011, pp. 1–8.

[4] J. He, Y. W. Li, and F. Blaabjerg, "Flexible Microgrid Power Quality Enhancement Using Adaptive Hybrid Voltage and Current Controller," *Industrial Electronics, IEEE Transactions on*, vol. 61, no. 6, pp. 2784–2794, June 2014.

[5] J. Zhang, D. Guo, F. Wang, Y. Zuo, and H. Zhang, "Control strategy of interlinking converter in hybrid AC/DC microgrid," in *Renewable Energy Research and Applications (ICRERA), 2013 International Conference on*, Oct 2013, pp. 97–102.

[6] M. Ambia, A. Al-Durra, and S. Muyeen, "Centralized power control strategy for AC-DC hybrid micro-grid system using multi-converter scheme," in *IECON 2011 - 37th Annual Conference on IEEE Industrial Electronics Society*, Nov 2011, pp. 843–848.

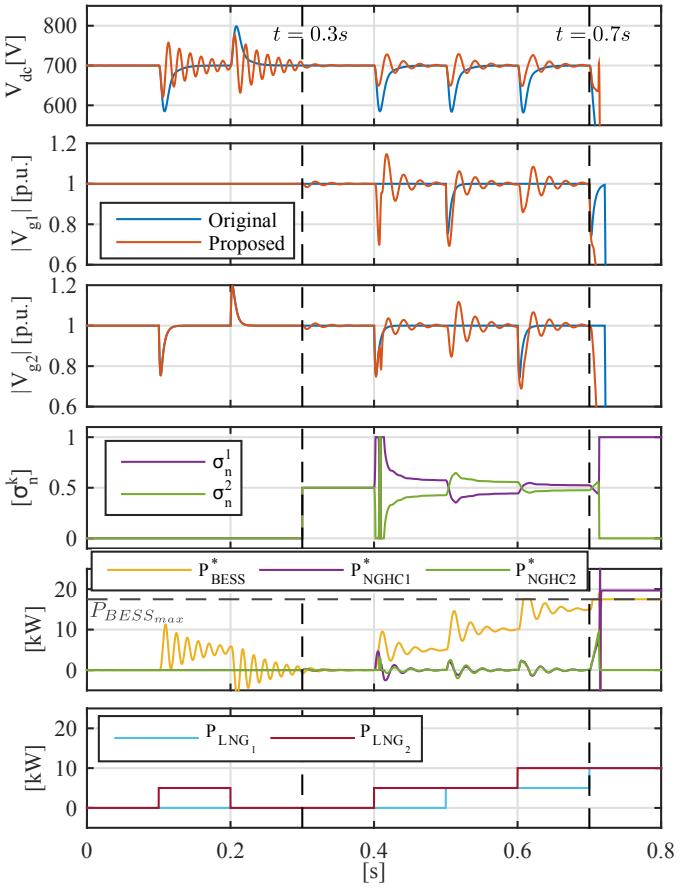

Fig. 9. Simulation results: Simulation results: performance using the proposed adaptive control method. Case 1: Without dynamic voltage compensator in the AC NGs. At t=0.3s the proposed adaptive mechanism is enabled. At t=0.7s the total load exceeds the maximum BESS available power, leading to global instability.

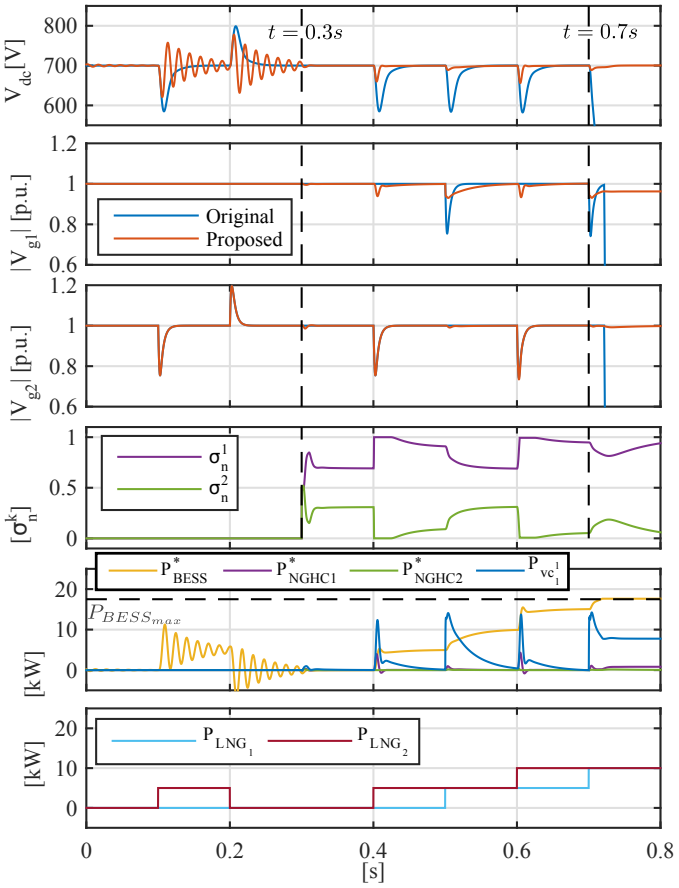

Fig. 10. Simulation results: performance using the proposed adaptive control method. Case 2: With dynamic voltage compensator in the AC NG 1 (Node B_1^1). At t=0.3s the proposed adaptive mechanism is enabled. At t=0.7s the total load exceeds the maximum BESS power and the compensator share the power during steady state.

[7] Y.-R. Mohamed and E. El-Saadany, "Adaptive Decentralized Droop Controller to Preserve Power Sharing Stability of Paralleled Inverters in Distributed Generation Microgrids," *Power Electronics, IEEE Transactions on*, vol. 23, no. 6, pp. 2806–2816, Nov 2008.

[8] M. Golsorkhi and D. Lu, "A Control Method for Inverter-Based Islanded Microgrids Based on V-I Droop Characteristics," *Power Delivery, IEEE Transactions on*, vol. 30, no. 3, pp. 1196–1204, June 2015.

[9] P. Arboleya, C. Gonzalez-Moran, and M. Coto, "A hybrid central-distributed control applied to microgrids with droop characteristic based generators," in *Power Electronics and Motion Control Conference (EPE/PEMC), 2012 15th International*, Sept 2012, pp. LS7a.5–1–LS7a.5–8.

[10] T. Dragievi, X. Lu, J. C. Vasquez, and J. M. Guerrero, "Dc microgrids-part i: A review of control strategies and stabilization techniques," *IEEE Transactions on Power Electronics*, vol. 31, no. 7, pp. 4876–4891, July 2016.

[11] D. Chen and L. Xu, "Autonomous dc voltage control of a dc microgrid with multiple slack terminals," *IEEE Transactions on Power Systems*, vol. 27, no. 4, pp. 1897–1905, Nov 2012.

[12] Z. Zhang, X. Huang, J. Jiang, and B. Wu, "A load-sharing control scheme for a microgrid with a fixed frequency inverter," *Electric Power Systems Research*, vol. 80, no. 3, pp. 311 – 317, 2010.

[13] A. Navarro-Rodriguez, P. Garcia, R. Georgious, and J. Garcia, "A communication-less solution for transient frequency drift compensation on weak microgrids using a D-statcom with an energy storage system," in *Energy Conversion Congress and Exposition (ECCE), 2015 IEEE*, Sept 2015, pp. 6904–6911.

[14] I. Serban and C. Marinescu, "Control Strategy of Three-Phase Battery Energy Storage Systems for Frequency Support in Microgrids and with Uninterrupted Supply of Local Loads," *Power Electronics, IEEE Transactions on*, vol. 29, no. 9, pp. 5010–5020, Sept 2014.

[15] M. Torres L, L. Lopes, L. Moran T, and J. Espinoza C, "Self-Tuning Virtual Synchronous Machine: A Control Strategy for Energy Storage Systems to Support Dynamic Frequency Control," *Energy Conversion, IEEE Transactions on*, vol. 29, no. 4, pp. 833–840, Dec 2014.

[16] Y. Hirase, O. Noro, K. Sugimoto, K. Sakimoto, Y. Shindo, and T. Ise, "Effects of suppressing frequency fluctuations by parallel operation of virtual synchronous generator in microgrids," in *Energy Conversion Congress and Exposition (ECCE), 2015 IEEE*, Sept 2015, pp. 3694–3701.

[17] L. Benadero, R. Cristiano, D. J. Pagano, and E. Ponce, "Nonlinear analysis of interconnected power converters: A case study," *IEEE Journal on Emerging and Selected Topics in Circuits and Systems*, vol. 5, no. 3, pp. 326–335, Sept 2015.

[18] T. Vandoorn, B. Renders, L. Degroote, B. Meersman, and L. Vandevelde, "Active Load Control in Islanded Microgrids Based on the Grid Voltage," *Smart Grid, IEEE Transactions on*, vol. 2, no. 1, pp. 139–151, March 2011, use of Voltage-droop control.

[19] M. K. Mishra and K. Karthikeyan, "A fast-acting dc-link voltage controller for three-phase dstatcom to compensate ac and dc loads," *IEEE Transactions on Power Delivery*, vol. 24, no. 4, pp. 2291–2299, Oct 2009.

[20] S. Vazquez, J. A. Sanchez, J. M. Carrasco, J. I. Leon, and E. Galvan, "A model-based direct power control for three-phase power converters," *IEEE Transactions on Industrial Electronics*, vol. 55, no. 4, pp. 1647–1657, April 2008.